Local and long range polar order in the relaxor-ferroelectric compounds $PbMg_{1/3}Nb_{2/3}O_3$ and $PbMg_{0.3}Nb_{0.6}Ti_{0.1}O_3$

B. Dkhil,[1] J. M. Kiat,[1,2] G. Calvarin,[1] G. Baldinozzi,[1] S. B. Vakhrushev,[3] and E. Suard[4]
[1]*Laboratoire Structures, Propriétés et Modélisation des Solides, CNRS-UMR 8580 Ecole Centrale Paris, 92295 Châtenay-Malabry cedex, France*
[2]*Laboratoire Léon Brillouin, CEN de Saclay, CEA-CNRS, 91191 Gif-sur-Yvette cedex, France*
[3]*Ioffe Phys-Tech. Institute RAS, 194021, 26 Politekhnicheskaya, St. Peterburg, Russia*
[4]*I.L.L., 6 rue Jules Horowitz, BP 156, 38402 Grenoble Cedex, France*
(Received 30 July 2001; published 17 December 2001)

Structural evolutions of PMN/PT10% ($PbMg_{0.3}Nb_{0.6}Ti_{0.1}O_3$) and PMN ($PbMg_{1/3}Nb_{2/3}O_3$) are studied and compared using high-resolution x-ray and neutron diffraction. At high temperature, PMN-like diffuse scattering, associated with local disordered shifts, is evidenced by PMN/PT10%. A part of this intensity condenses at $T_c = 285$ K when PMN/PT10% exhibits a structural phase transition toward a long-range rhombohedral phase, whereas in PMN the polar order remains short ranged. In the ferroelectric phase of PMN/PT10% local [100] displacements of lead are evidenced, and are connected to the observation of diffuse scattering far below T_c. The local symmetry in which oxygen and Ti/Mg/Nb cations are shifted along the [111] direction, but in which the lead atoms are shifted along one of the tetragonal [100] directions is monoclinic. This short-range polar order reconstructs on average a polar rhombohedral symmetry. A global picture for the structural evolution in the PMN/PT compounds is proposed. It is based on competition between rhombohedral and tetragonal polar order, which connects the relaxation properties of PMN and the high piezoelectric response of morphotropic monoclinic PMN/PT with a high concentration of PT.

DOI: 10.1103/PhysRevB.65.024104 PACS number(s): 77.84.Dy, 77.80.Bh, 77.90.+k, 61.10.−i

I. INTRODUCTION

The complex perovskite lead magnoniobate $PbMg_{1/3}Nb_{2/3}O_3$ (PMN) belongs to the relaxor ferroelectric family, and is considered to be the prototype compound for fundamental scientific understanding. In addition, PMN-related materials display high dielectric constants, strong pyroelectric and piezoelectric coefficients, or giant electrostriction, which make them of a great interest for advanced technologies.[1] The main feature of a relaxor is a large dielectric permittivity (for PMN, $\varepsilon' = 20\,000$ at $T_{max} = 265$ K and $f = 1$ kHz) (Ref. 2) over a wide temperature range with a significant frequency relaxation. The relaxation phenomenon is essentially observed on lead-based complex perovskite $PbBB'O_3$ with the B site occupied by at least two different valence cations. Contrary to a normal ferroelectric, the dielectric anomaly is not directly linked to a structural phase transition in PMN, as evidenced by x-ray and neutron-diffraction studies, because the average symmetry of this compound remains cubic whatever the temperature is.[3,4] However, diffuse scattering in the neutron- and x-ray-diffraction patterns is observed, and has been interpreted by the existence of polar nanometric regions with possibly rhombohedral symmetry, resulting from short-range correlated atomic shifts, and whose size freezes below T_f, the freezing temperature ($T_f \approx 220$ K).[5] The dielectric relaxation was therefore explained to arise from a size distribution of these polar regions.

On the other hand, it is possible to induce a phase transition in PMN by application of a static external electric field[6,7] and the associated nucleation and growth of the ferroelectric phase induces strong kinetic effects.[8–10] The electric-field-induced phase has a rhombohedral symmetry, which is consistent with the structural hypothesis of short ranged rhombohedral polar regions in unpoled PMN.

Another way[11] to induce long-range polar ferroelectric ordering in PMN is to substitute Mg^{2+}/Nb^{5+} with Ti^{4+} by addition to PMN relaxor of $PbTiO_3$ (PT), a true ferroelectric. The $(1-x)PMg_{1/3}Nb_{2/3}O_3/xPbTiO_3$ (PMN/PT) solid solutions obtained, with $0 \leqslant x \leqslant 1$, exhibit various ferroelectric properties depending on x concentration.

In low PT content ($x \leqslant 0.13$), dielectric and electromechanical properties at room temperature are typical of a relaxor behavior, and the average crystal structure is then considered to be pseudocubic like pure PMN.[12] These results are consistent with x-ray studies of $x = 0.05$ and 0.1 single crystals[13] and optical studies of PMN/PT10% single crystal.[14] Nevertheless in the relaxor composition PMN/PT7%, an instantaneous transformation into a complex array of ferroelectric macrodomains was observed by TEM and attributed to the irradiation due to the electron beam.[15] Moreover, a spontaneous rhombohedral-cubic phase transition was reported at 290 K in a PMN/PT10% ceramic sample.[16] It then seems that there is a need of clarification concerning the structural situation of PMN/PT10% compound.

One puzzling point in the structural interpretation of the dielectric relaxation is the fact that the observation of long ranged polar order in PMN/PT does not result in the disappearance of this relaxation. Indeed when increasing the PT content in a PMN/PT solid solution, the dielectric constant becomes sharper, and a clear spontaneous rhombohedral-cubic phase transitions occur for $x \geqslant 0.2$[11], but dielectric relaxation is observed up to 30% content of Ti. In the same manner, dielectric relaxation is also observed in the field-induced ferroelectric phase of PMN. Setter and Cross reported a spontaneous ferroelectric long-range order in re-

laxor PST and PSN,[17] which definitively showed that the interpretation of dielectric relaxation based on short ranged polar order was simplistic (also see Malibert *et al.*[18]). In PMN/PT for $x \geqslant 0.4$, a classical temperature dependence of the dielectric constant is recovered, similar to pure PT, with a phase transition from a cubic phase to a tetragonal phase. The intermediate region around $x=0.35$, called the morphotropic phase region by analogy with the well-known system $PbZr_{1-x}Ti_xO_3$ (PZT), is characterized by ultrahigh piezoelectric response. These unusual properties were supposed to result from the local texture of the adjacent rhombohedral and tetragonal competing phases.[11] However, based on recent theoretical considerations[19–21] and experimental discovery of a (*Cm*) monoclinic phase in ultrahigh piezoelectric systems such as PZT (Refs. 22 and 23) and poled $92\%PbZn_{1/3}Nb_{2/3}O_3/8\%PbTiO_3$,[24] an other monoclinic phase was evidenced in PMN/PT35% and unpoled $90\%PbZn_{1/3}Nb_{2/3}O_3/10\%PbTiO_3$.[25] This last unpoled monoclinic phase is characterized by a (*Pm*) space group with a polarization inside the pseudocubic (100) plane, i.e., between the [001] tetragonal direction and the [011] orthorhombic direction, allowing the rotation of this polarization between the two adjacent phases when the Ti concentration is changed.

Recently, Blinc and co-workers proposed to explain relaxor features of a spherical random bond random field model[26,27] which incorporates the previous models; the dipole glass (random bond) model[28] and the random field (or pinning) model,[29,30] in a self-consistent manner. In this hybrid model, the dynamic of the polarization is controlled by the random/spherical bond characteristics, which are induced by random fields. Multiple competing orderings of the polarization along multiple directions are allowed. Such an approach allows for a sophisticated understanding of competing interactions on a mesoscale. Obtaining an atomic level picture of competing interactions should therefore be help in understanding.

The purpose of this investigation is to study the structural evolution of the ferroelectric relaxor PMN/PT10% compound, and to compare it with PMN using a combination of x-ray and neutron diffraction on single-crystal and powder samples. A global picture for the structural evolution in the PMN/PT compounds is proposed. It is based on the competition between rhombohedral and tetragonal polar orders which connects the relaxation properties of PMN and the high piezoelectric response of morphotropic monoclinic PMN/PT.

II. EXPERIMENTS

A powdered PMN/PT10% sample was synthesized by the Swartz-Shrout method.[31] A single crystal with the same Ti^{4+} composition and a PMN single crystal both with large faces oriented along the [100] direction were grown by the flux method.

The x-ray diffraction was performed with a high accuracy 2-axis diffractometer (Bragg-Brentano geometry) equipped with a rotating anode generator of 18 kW, using a cryofurnace between 473 and 80 K. The neutron single-crystal diffraction was performed at $T=300$ K ($\lambda=0.9$ Å) with $\sin\theta/\lambda$ up to 0.95 $Å^{-1}$ (74 equivalent reflections) using a 6T2 four-circle diffractometer, and the neutron powder diffraction patterns were recorded at $T=80$ and 523 K ($\lambda=1.227$ Å) with $\sin\theta/\lambda$ up to 0.73 $Å^{-1}$ using steps of 0.05° between 6 and 120° 2θ, with a 3T2 powder diffractometer using the Orphée reactor facilities on a thermal source at Laboratoire Léon Brillouin (Saclay, France). A collection of neutron powder diffraction patterns between 100 and 900 K was also performed using the high flux at $\lambda=2.52$ Å with a 80° multidetector of *D1B* two-axis diffractometer at Institut Laüe Langevin (Grenoble, France). Powder refinements based on Rietveld method have been performed with XND software[32] and the single crystal refinements with SHELXL-98 program.[33]

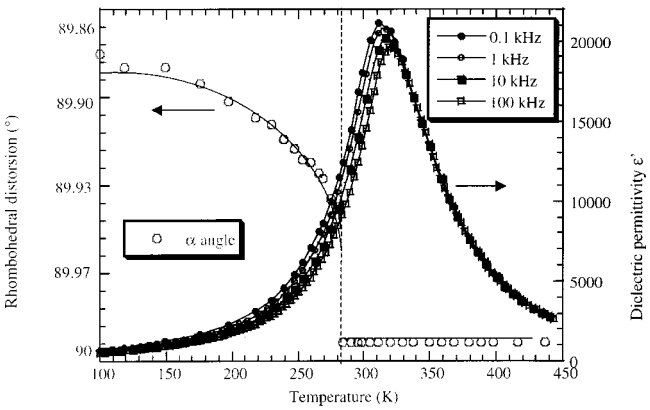

FIG. 1. Dielectric permittivity at different frequencies vs the temperature of the PMN/PT 10% ceramic sample, and the rhombohedral distortion vs temperature obtained from (222) Bragg reflection on the same sample.

III. RESULTS

A. Phase transition and dielectric properties of PMN/PT10%

The PMN/PT10% ceramic exhibits a strong value of the dielectric constant ε' (Fig. 1) over a wide temperature range with a dielectric relaxation ($T_{max}=315$ K at $f=1$ kHz) similar to the one observed for PMN. However, x-ray-diffraction patterns reveal a first-order phase transition which takes place at $T_c=285(5)$ K from a cubic paraelectric phase to a rhombohedral ferroelectric phase. The (222) Bragg reflection splitting (left of Fig. 2) allowed us to extract the rhombohedral distortion α versus temperature (Fig. 1). This result clearly shows that, from a structural point of view, PMN/PT10% behaves differently from pure PMN, in which the polar order remains only short ranged. Furthermore, no anomaly on ε' is detected around T_c in either ceramic or single crystal samples, and the dielectric relaxation exists in both parts, above and below T_c temperature (Fig. 1).

In addition, the high-resolution x-ray-diffraction pattern reveals diffuse scattering, particularly strong close to $\{h00\}$ with odd h Bragg reflections (right of Fig. 2). From (300) $\theta/2\theta$ scans, we extracted the temperature dependence of Bragg and diffuse scattering contribution. Figure 3 shows a comparison of the temperature dependence of the diffuse intensity and of the lattice parameter associated with the (300)

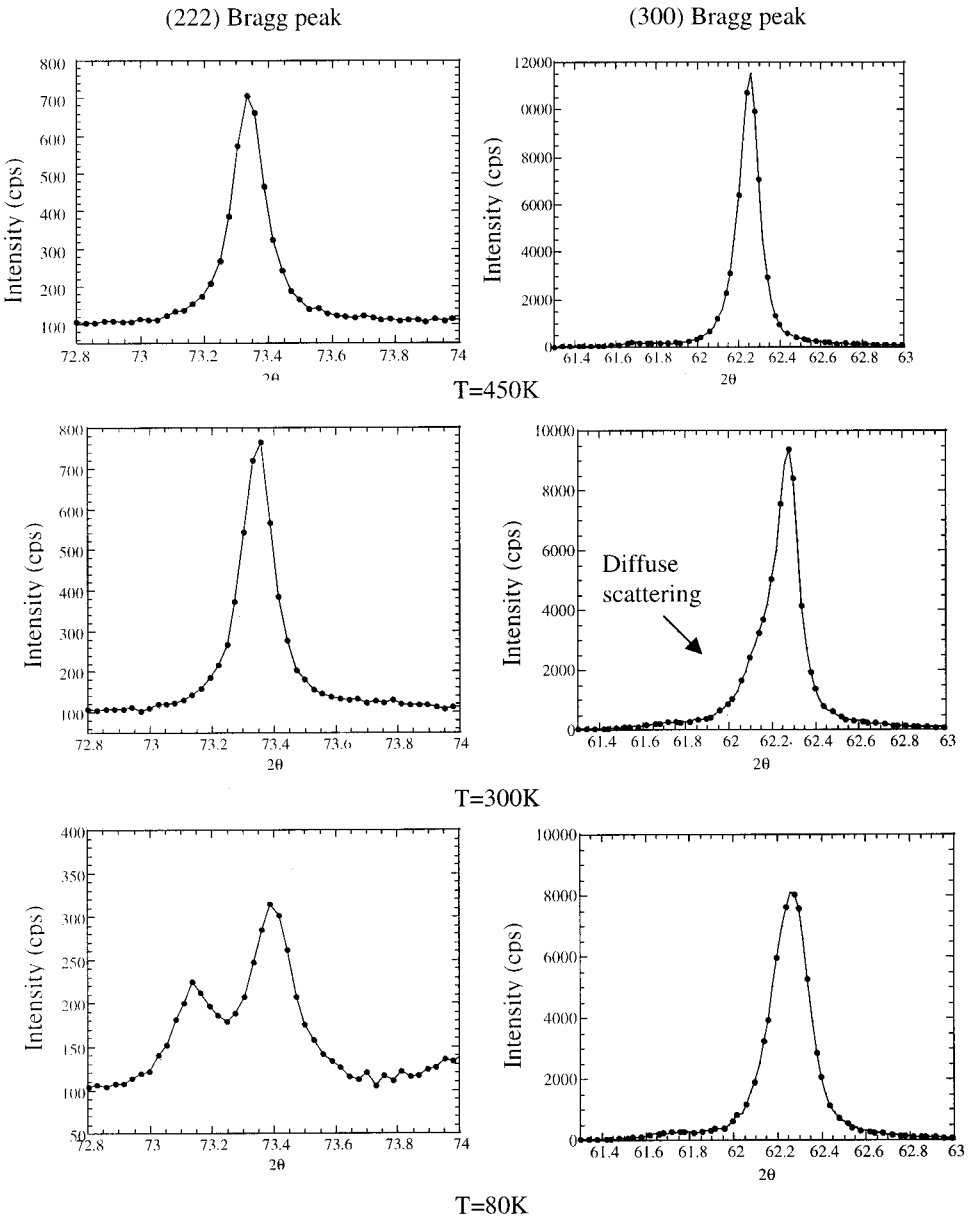

FIG. 2. Left: (222) Bragg peak. Right: (300) Bragg peak. (From x-ray diffraction.)

peak, which behave very differently in PMN and PMN/PT10%. Indeed, in PMN on cooling from high temperature the diffuse intensity is detected at $T_L \approx 350$ K, and increases and saturates below $T_f = 200$ K, with corresponding anomalies in the lattice parameter evolution, whereas in PMN/PT10% the diffuse intensity, detected next to 350 K, increases, displays a critical divergence at $T_c = 285$ K, but does not vanish to zero below T_c. It reaches a temperature-independent value below $T_f = 240$ K. The lattice cell parameter of PMN/PT10% shows anomalies at T_c, T_f, and $T_L \approx 400$ K, corresponding to a deviation to the linear evolution.

(111) and (210) reflections have been measured in PMN/PT10% by neutron-diffraction between 100 and 900 K (Fig. 4). In this experiment, diffuse and Bragg diffraction intensity contributions are not separated due to poorer resolution compared to x-ray experiments. The integrated intensity displays a slope change at $T_L \approx 400$ K, which shows that structural modifications occur in the high-temperature averaged cubic structure. This change is stronger for (210) peak than for the (111) peak which is known to be less sensitive to the diffuse scattering.[3–5] The phase transition is expressed by a weaker anomaly at $T_c = 285$ K.

B. Structural evolution of PMN/PT10%

In order to clarify the structural evolution, we have performed three data collections: two in the cubic phase at $T = 523\,\mathrm{K} > T_L$ (powder) and at $T_c < T = 300\,\mathrm{K} < T_L$ (single crystal), and another one in the rhombohedral phase at $T = 80$ K (powder).

1. Structure of the high-temperature cubic phase at $T = 523$ K ($T > T_L > T_c$)

As a starting model for a refinement of the neutron powder diffraction pattern, the ideal cubic perovskite (space

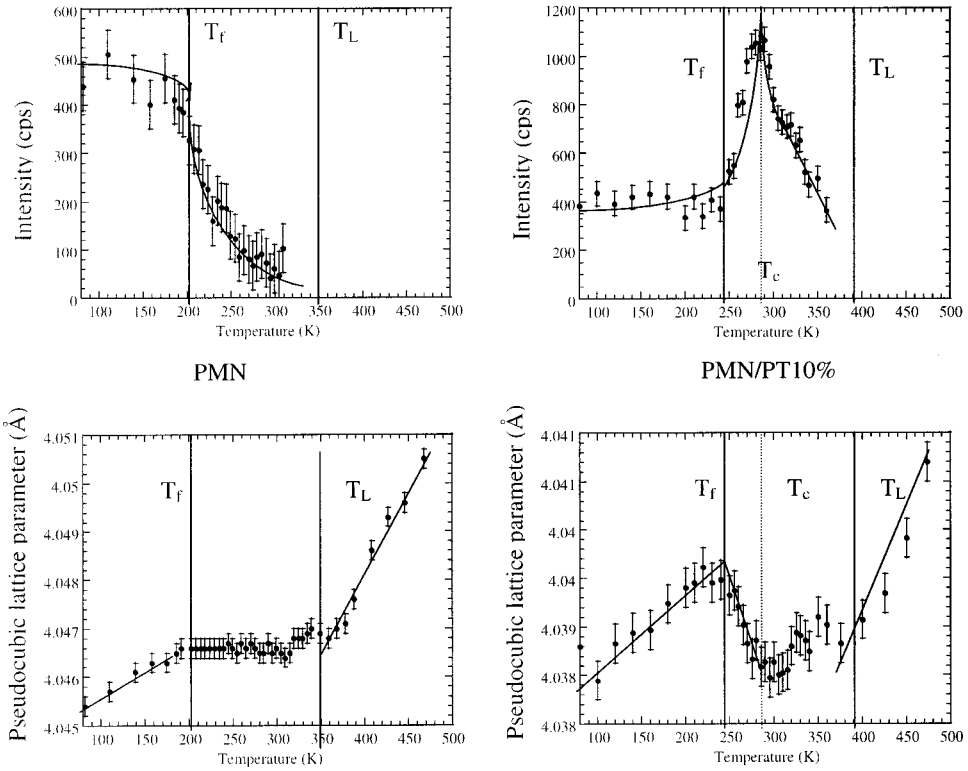

FIG. 3. Temperature evolution of the intensity of the diffuse scattering (top) and the pseudocubic lattice parameter (bottom) for a PMN single crystal (on the left) and a PMN/PT 10% single crystal (on the right) [from the (300) Bragg peak]. Curves are to guide the eyes.

group $Pm\bar{3}m$) was taken with the atoms fixed at their special Wyckoff positions. As the atoms Mg, Nb, and Ti are randomly distributed over the perovskite *B* site, we have classically considered an averaged atom on this site.

The refinement was first carried out with individual isotropic temperature factors B^{iso}. Although satisfactory agreement factors ($R_{\mathrm{wp}}=4.73\%, R_{\mathrm{B}}=3.43\%, Gof=1.67$) were achieved, B^{iso} for O and for Pb are very large [$B_0^{\mathrm{iso}}=1.75(1)$ Å^2 and $B_{\mathrm{Pb}}^{\mathrm{iso}}=3.99(2)$ Å^2], much larger than B^{iso} for Mg/Nb/Ti [$B_{\mathrm{Mg/Nb/Ti}}^{\mathrm{iso}}=0.81(1)$ Å^2], which is a normal value. Such high B^{iso} values for O and Pb in lead-based perovskites are well known in the literature ($Pb/Mg_{1/3}Nb_{2/3}O_3$,[5,34] $PbSc_{1/2}Nb_{1/2}O_3$,[18] $PbZn_{1/3}Nb_{2/3}O_3$/9%$PbTiO_3$,[35] $PbFe_{1/2}Nb_{1/2}O_3$,[36] etc.), and are usually ascribed to local disordered displacements (static and/or dynamic).

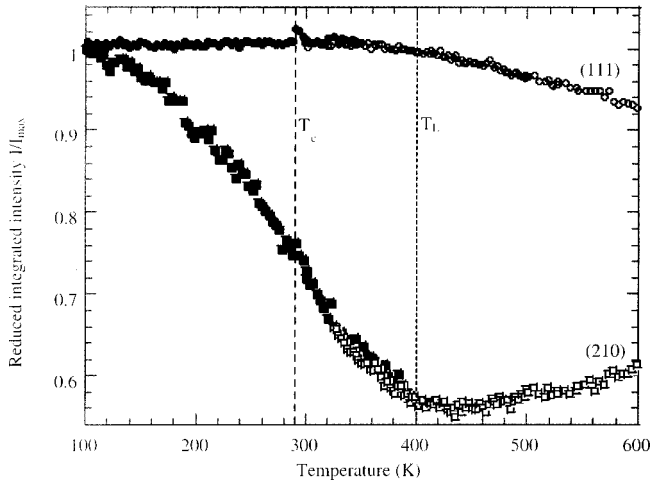

FIG. 4. Integrated intensity of (111) and (210) Bragg peak reflection vs temperature (from neutron diffraction).

Refinement with anisotropic temperature factors assigned to O gave an improved fit ($R_{\mathrm{wp}}=3.60\%$ and $R_B=1.94\%$) with the mean-square displacement $\sqrt{\langle u_{11}\rangle^2}=\sqrt{\langle u_{22}\rangle^2}=0.164(1)$ Å larger than $\sqrt{\langle u_{33}\rangle^2}=0.062(1)$ Å corresponding to vibrations mainly within the faces of the cubic cell. This disk-shaped thermal ellipsoid of O atoms, which points out dynamic and/or static displacements with an amplitude in the {110} plane much more stronger than along the B-O-B bonds in the ⟨110⟩ perpendicular direction is also well known. Such an anisotropy can be interpreted as a result of low-frequency tilts of the oxygen octahedron.[37] However, a static component for these anomalous B parameter certainly arises from the existence of the random distribution of the cations on the Ti/Mg/Nb site. Indeed, the size of oxygen octahedron surrounding Nb^{5+} cation should be different to the size of the octahedron containing Mg^{2+} or Ti^{4+}.

In the next stage of our refinement, we have supposed a Pb atom located in a multiwelled potential around its special Wyckoff position. In this purpose, we have applied a commonly used procedure[38] consisting of a series of refinements in which the agreement factor R_B is plotted as a function of Pb atom shift δ_{Pb} with only the thermal factor *B* varying and all the other parameters fixed. By this way, we avoid strong correlations between the shift and the *B* factor. Four kinds of Pb disorder directions have been tested—⟨100⟩, ⟨111⟩, ⟨110⟩, and ⟨123⟩—corresponding, respectively, to 6, 8, 12, and 48 equivalent directions in the cubic symmetry. Figure 5 shows that there is a well-defined minimum in the R_B factor for a displacement of about $\delta_{\mathrm{Pb}}=0.27(2)$ Å whatever the tested

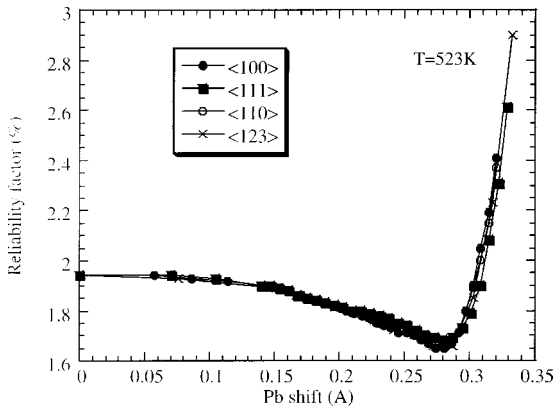

FIG. 5. Reliability factor R as a function of Pb shift in different directions at $T=523$ K. Neutron data (sin θ/λ up to 0.95 Å^{-1}).

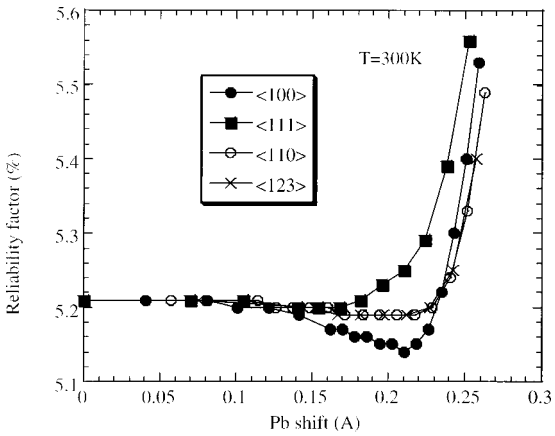

FIG. 6. Reliability factor R as a function of Pb shift in different directions at $T=300$ K. Neutron data (sin θ/λ up to 0.95 Å^{-1}).

directions. In this minimum, the B factor recovers a more normal value of $B_{\mathrm{Pb}}^{\mathrm{iso}}=1.7(1)$ Å^2. These multiple-welled solutions indicate in fact, as we have discussed in Ref. 39, spherical shell-shaped positions for lead which can be evidenced via anharmonic refinements based on Gram-Charlier expansion of thermal parameter determination when very high sin θ/λ (up to 2.5 Å^{-1}) data are available.[39]

2. Structure of the relaxor state at $T=300$ K ($T_c<T<T_L$)

We have performed a structural refinement at $T=300$ K, at a temperature close to $T_{\max}$ and just above T_c. The structure can be satisfactorily ($R=5.21\%$) refined with the high-temperature cubic phase $Pm\bar{3}m$ space group and thermal B parameters of $B_{\mathrm{Pb}}=3.98(22)$ Å^2 and $B_{\mathrm{O}}=1.73(9)$ Å^2, again with a disk-shaped thermal ellipsoid with $\sqrt{\langle u_{11}\rangle^2}=\sqrt{\langle u_{22}\rangle^2}=0.161(1)$ Å larger than $\sqrt{\langle u_{33}\rangle^2}=0.121(1)$ Å and $B_{\mathrm{Mg/Nb/Ti}}=0.79(10)$ Å^2. Still B_{Pb} and B_{O} factors are strong.

In a similar way as done in the high-temperature cubic phase we have performed some tests of disorder positions for Pb atom for different directions. The results are clearly different from those obtained at high temperature. Indeed the $\langle 111\rangle$ shifts model is now clearly rejected by the refinement and only the $\langle 100\rangle$ sixfold direction displays a clear minimum of the agreement factor $R=5.14\%$ for about $\delta_{\mathrm{Pb}}\approx 0.21$ Å (Fig. 6), the value for which B_{Pb} recovers a value of 2.8(1) Å^2. One can also note that the $\langle 111\rangle$ shifts model is clearly rejected by the refinement.

TABLE I. Refinement results obtained in the ferroelectric phase at $T=80$ K with a Pb disorder in plane perpendicular to the [111] polar axis.

Lattice cell parameters		4.039(1)
α (°)	a_r (Å)	89.87(1)
Pb position	$\delta_{\mathrm{Pb}}^{\perp}$ (Å)	0.239(1)
B_{iso}(Pb) (Å^2)		0.67(5)
B_{eq}(Pb) (Å^2) when $\delta_{\mathrm{Pb}}^{\perp}=0$		2.24
Mg/Nb/Ti position	$x=y=z$	0.5290(4)
β_{11}		0.0069(4)
β_{12}		−0.0025(17)
B_{eq} (Mg/Nb/Ti) (Å^2)		0.45
O position	$x=y$	0.5444(7)
z		0.0350(8)
β_{11}		0.0221(6)
β_{33}		0.0111(6)
β_{12}		0.0034(25)
β_{13}		0.0201(18)
B_{eq}(O) (Å^2)		1.21
Reliability factors R_{wp} (%)		5.96
R_{Bragg} (%)		3.20
Gof		2.19

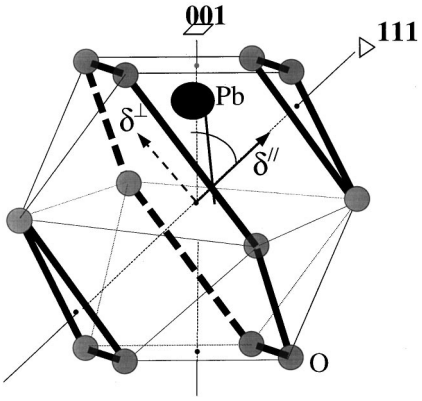

FIG. 7. Pb atom position in its oxygen cuboctahedron.

3. Structure of the ferroelectric phase at $T=80\,K$ ($T<T_c$)

At $T=80\,\mathrm{K}$, the structure is satisfactorily refined ($R_{wp}=5.96\%$, $R_B=3.20\%$, and $Gof=2.19$) in the $R3m$ symmetry. In this noncentrosymmetric spatial group, we have fixed the lattice origin (0,0,0) on the Pb atom, as commonly used in perovskite structure descriptions. Mg/Nb/Ti and O atoms have the positions $(1/2+\varepsilon,1/2+\varepsilon,1/2+\varepsilon)$ and $(1/2+\varepsilon',1/2+\varepsilon',\varepsilon'')$, $(1/2+\varepsilon',\varepsilon'',1/2+\varepsilon')$, $(\varepsilon'',1/2+\varepsilon',1/2+\varepsilon')$, respectively, with $\varepsilon'=\varepsilon''$ if the oxygen polyhedra (octahedra and cuboctahedra) remain undistorted.

The results of the final refinement are summarized in Table I. In this ferroelectric phase the lead atom and the cation Mg/Nb/Ti are now out off the center of the oxygen polyhedron along the [111] threefold polar axis. The ferroelectric phase is characterized by weak displacements for the Mg/Nb/Ti cation ($\delta^{\parallel}_{\mathrm{Mg/Nb/Ti}}=0.05$ Å compared to $\delta^{\parallel}_{\mathrm{Pb}}=0.27$ Å, where the δ's are shifts of the cations from the barycenter of the O atoms) and a small distortion of the oxygen polyhedra ($\varepsilon'=0.0444\neq\varepsilon''=0.0350$, three short B-O bonds [2.800(3) Å], and three long B-O bonds [2.894(3) Å]).

The strong value for the lead atom thermal factor ($B_{\mathrm{Pb}}=2.24\,\mathrm{Å}^2$) is again an indication of disorder from average positions. In addition to the cooperative shift of $\delta^{\parallel}_{\mathrm{Pb}}=0.27$ Å for a Pb atom along the polar [111] axis we have tested disordered shifts, according to the procedure used in Sec. II B 2; however, due to the cooperative shifts along the [111] direction which break the cubic symmetry, it is not possible to test directly disordered ⟨100⟩-like shifts. Instead we have tested ⟨2-1-1⟩-type directions which are perpendicular to the [111] axis and which form, with the [111] axis, a plane containing [100] direction: additional local shifts $\delta^{\perp}_{\mathrm{Pb}}=0.239$ Å (Fig. 7) were evidenced through R_B minima, for which the Pb thermal factor recovers a normal value of 0.67(5) Å^2 (Table II). The composition of cooperative shifts along the [111] polar direction with short-range shifts along the [2-1-1] direction gives the local position of the lead atom inside the rhombohedral cell, which deviates slightly from the pseudocubic [100] direction ($\approx 14°$).

IV. DISCUSSION AND CONCLUSION

X-ray and neutron diffraction have allowed us to show that PMN/PT10% displays a structural phase transition at $T_c=285(5)$ K from a cubic phase to a rhombohedral phase with a distortion $\alpha=89.87°$ at $T=80$ K, comparable to a distortion of the field-induced phase of PMN.[40] However, local deviations from the average structure were proven through large thermal factors which were modeled by introducing short-range shifts from atomic sites, and through an observation of diffuse scattering.

At high temperature ($T>T_L$), the structural refinements of the cubic phase showed that it is usually a disorder of positions for Pb atoms which are randomly distributed over a sphere centered on a Pb atom special site. When the temperature is lowered, the appearance of diffuse scattering at a temperature close to T_L, as well as anomalies in the temperature-dependence of the $(h00)$ lattice parameter and of neutron Bragg peaks intensities, indicate the progressive growth of local correlations, which finally diverge at T_c, a temperature below which a long-range ferroelectric rhombohedral phase is established.

However, two-diffraction experimental results show at least, in addition to the dielectric behavior, a more complex mechanism for this phase transformation than a classic displacive/order-disorder mechanism. First, inside a cubic phase close to T_c the structural refinements clearly show that locally the lead atom is out of its symmetry site, along the ⟨100⟩ directions, and that these short-range shifts are also observed inside the rhombohedral phase: the rhombohedral symmetry is only an average symmetry. Such a local Pb displacement along the [100] direction was already reported in the rhombohedral phase of $PbSc_{1/2}Ta_{1/2}O_3$ (PST), using pair-density function analysis,[41] and in PSN.[18] Second, in addition to the critical scattering, PMN-like diffuse scattering, which does not condense at T_c which and has no temperature dependence below $T_f=240$ K, is observed down to the rhombohedral phase.

A possible global picture for both PMN and PMN/PT systems, based on a competition between rhombohedral and tetragonal orders could be as follows. At high temperature the shifts of lead along a spherical shell are noncorrelated from one cell to another cell. Upon cooling, correlations appear and are detected in our experiments at T_L. However two local orderings are competing: (1) a polar tetragonal order in which some atoms (Pb) are shifted along the [100] direction, and (2) a polar rhombohedral order in which other atoms (O and Ti/Mg/Nb) are shifted along the [111] direction. In pure PMN none of these polar orders becomes long ranged: indeed, the diffuse scattering displays no critical behavior but a freezing below T_f. In PMN/PT10%, both freezing and critical behaviors are observed, and a long-range rhombohedral order is established at low temperature. However the [111] direction of displacements is only an average direction, for the lead atoms which are rather shifted in a ⟨100⟩-type direction inside a unit cell.

From a chemical point of view the ⟨100⟩ direction of the shift corresponds to a lead atom displacement in its oxygen cuboctahedron toward four of its oxygen neighbors (Fig. 7). This shift is the most chemically favored one, and is observed in $PbTiO_3$ or PbO, it is a consequence of the existence of the lone pair electrons in PbO.[42] In this cubic to rhombohedral phase transition, the Pb atoms receive a reduction of

the number of their disordered positions from 6 in the cubic phase to 3 in the low temperature phase: this points out an order-disorder aspect for the phase transition.

The local symmetry in which oxygen and Ti/Mg/Nb cations are shifted along the [111] direction, but in which the lead atoms displacements are correlated along one of the ⟨100⟩ directions, is therefore monoclinic. In this picture, this monoclinic symmetry is only a short-ranged one, whereas the long-range structure remains rhombohedral in average.

When increasing the titanium content up to morphotropic concentrations a long, range polar monoclinic order is established, as we recently reported,[25] in PMN/PT35%, in a small range of concentration, instead of the rhombohedral order. At a macroscopic level, this monoclinic phase allows the polarization rotation between the tetragonal phase (high titanium concentration region) and the rhombohedral phase (low titanium concentration region), in accordance with theoretical considerations of Fu and Cohen[21] and Vanderbilt and Cohen.[43] At higher concentration of titanium, a $PbTiO_3$-type tetragonal phase is established.

In both cubic and rhombohedral phases, the strong off-center positions of Pb induce large dipolar moments. When correlations start to grow, a mesoscale polarization appears. Observation of dielectric relaxation below and above T_c in PMN/PT10% and in PMN could be a consequence of competing rhombo/tetra ordering of Pb atoms in the form of small monoclinic (rather than rhombohedral) polar regions with size distributions.

This picture of course has to be checked and completed from several points of view. In particular, the competition between rhombohedral and tetragonal local order may be associated with two competing soft modes. In this framework inelastic measurements in PMN have revealed a complex situation with the existence of a central peak with two maxima in its temperature dependence,[44] and a strong quasioptic excitation.[45] In this picture we have also neglected the part played by the well-known local chemical ordering[15] associated with a $\frac{1}{2}$-$\frac{1}{2}$ composition, which is obviously important because possibly associated random fields have been shown to prevent the long-range polar order in PMN in the random-bond–random-field model of Blinc *et al.*[26]

[1] L. E. Cross, Ferroelectrics **76**, 241 (1987).
[2] G. A. Smolenskii *et al.*, Fiz. Tverd. Tela (Leningrad) **2**, 2906 (1960) [Sov. Phys. Solid State **2**, 2584 (1961)].
[3] P. Bonneau, P. Garnier, E. Husson, and A. Morell, Mater. Res. Bull. **24**, 201 (1989).
[4] P. Bonneau, P. Garnier, G. Calvarin, E. Husson, J. R. Gavarri, A. W. Hewat, and A. Morell, J. Solid State Chem. **91**, 350 (1991).
[5] N. de Mathan, E. Husson, G. Calvarin, J. R. Gavarri, A. W. Hewat, and A. Morell, J. Phys.: Condens. Matter **3**, 8159 (1991).
[6] H. Arndt, F. Sauerbier, G. Schmidt, and L. A. Shebanov, Ferroelectrics **79**, 145 (1988).
[7] G. Calvarin, E. Husson, and Z. G. Ye, Ferroelectrics **165**, 349 (1995).
[8] S. B. Vakhrushev, J. M. Kiat, and B. Dkhil, Solid State Commun. **103**, 477 (1997).
[9] K. Fujishiro, Y. Uesu, Y. Yamada, B. Dkhil, J. M. Kiat, and Y. Yamashita, J. Korean Phys. Soc. **32**, S964 (1998).
[10] B. Dkhil and J. M. Kiat, J. Appl. Phys. **90**, 4676 (2001).
[11] O. Noblanc, P. Gaucher, and G. Calvarin, J. Appl. Phys. **79**, 4291 (1996).
[12] S. J. Jang, K. Uchino, S. Nomura, and L. E. Cross, Ferroelectrics **27**, 31 (1980).
[13] O. Bunina, I. Zakharchenko, S. Yemelyanov, P. Timonin, and V. Sakhnenko, Ferroelectrics **157**, 299 (1994).
[14] K. Fujishiro, T. Iwase, Y. Uesu, Y. Yamada, B. Dkhil, J. M. Kiat, S. Mori, and N. Yamamoto, J. Phys. Soc. Jpn. **69**, 2331 (2000).
[15] A. D. Hilton, C. A. Randall, D. J. Barber, and T. R. Shrout, Ferroelectrics **93**, 379 (1989).
[16] O. Bidault, M. Licheron, E. Husson, G. Calvarin, and A. Morell, Solid State Commun. **98**, 765 (1996).
[17] N. Setter and L. E. Cross, J. Mater. Sci. **15**, 2478 (1980).
[18] C. Malibert, B. Dkhil, J. M. Kiat, D. Durand, J. F. Bérar, and A. Spasojevic-de-Biré, J. Phys.: Condens. Matter **9**, 7485 (1997).
[19] A. Garcia and D. Vanderbilt, Appl. Phys. Lett. **72**, 2981 (1998).
[20] L. Bellaiche, A. Garcia, and D. Vanderbilt, Phys. Rev. Lett. **84**, 542 (2000).
[21] H. Fu and R. E. Cohen, Nature (London) **403**, 281 (2000).
[22] B. Noheda, J. A. Gonzalo, L. E. Cross, R. Guo, S. E. Park, D. E. Cox, and G. Shirane, Phys. Rev. B **61**, 8687 (1999).
[23] R. Guo, L. E. Cross, S. E. Park, B. Noheda, D. E. Cox, and G. Shirane, Phys. Rev. Lett. **84**, 5423 (2000).
[24] B. Noheda, D. E. Cox, G. Shirane, S. E. Park, L. E. Cross, and Z. Zhong, Phys. Rev. Lett. **86**, 3891 (2001).
[25] J. M. Kiat, Y. Uesu, B. Dkhil, M. Matsuda, C. Malibert, and G. Calvarin, Phys. Rev. B (to be published).
[26] R. Blinc, J. Dolinsek, A. Gregorovic, B. Zalar, C. Filipic, Z. Kutnjak, A. Levstik, and R. Pirc, J. Phys. Chem. Solids **61**, 177 (2000).
[27] V. Bobnar, Z. Kutnjak, R. Pirc, R. Blinc, and A. Levstik, Phys. Rev. Lett. **84**, 5892 (2000).
[28] D. Viehland, S. J. Jang, L. E. Cross, and M. Wuttig, J. Appl. Phys. **68**, 2916 (1990).
[29] V. Westphal, W. Kleemann, and M. J. Glinchuk, Phys. Rev. Lett. **68**, 847 (1992).
[30] W. Kleemann, Int. J. Mod. Phys. **7**, 2469 (1993).
[31] S. L. Swartz and T. R. Shrout, Mater. Res. Bull. **17**, 1245 (1982).
[32] J. F. Bérar and G. Baldinozzi, CPD Newsletter **20**, 3 (1998).
[33] G. M. Sheldrick, (1993) SHELX93, Program for crystal structures refinement, University of Göttingen, Germany.
[34] S. G. Zhukov, V. V. Chernishev, L. A. Aslanov, S. B. Vakhrushev, and H. Schenk, J. Appl. Crystallogr. **28**, 385 (1995).
[35] Y. Uesu, Y. Yamada, K. Fujishiro, H. Tazawa, S. Enokido, J. M. Kiat, and B. Dkhil, Ferroelectrics **217**, 319 (1998).
[36] N. Lampis, P. Sciau, and A. Geddo Lehmann, J. Phys.: Condens. Matter **11**, 3489 (1999).
[37] W. Hewat, J. Phys. C **6**, 2559 (1973).
[38] G. Shirane, J. D. Axe, J. Harada, and J. P. Remeika, Phys. Rev. B **2**, 155 (1970).

[39] J. M. Kiat, G. Baldinozzi, M. Dunlop, C. Malibert, B. Dkhil, C. Ménoret, O. Masson, and M. T. Fernandez-Diaz, J. Phys.: Condens. Matter **12**, 8411 (2000).
[40] N. de Mathan, E. Husson, G. Calvarin, and A. Morell, Mater. Res. Bull. **26**, 1167 (1991).
[41] W. Dmowski, M. K. Akbas, P. K. Davies, and T. Egami, J. Phys. Chem. Solids **61**, 229 (2000).
[42] D. Le Bellac, J. M. Kiat, and P. Garnier, J. Solid State Chem. **114**, 459 (1995).
[43] D. Vanderbilt and M. H. Cohen, Phys. Rev. B **63**, 094108 (2001).
[44] I. G. Siny, S. G. Lushnikov, and R. S. Katiyar, Phys. Rev. B **56**, 7962 (1997).
[45] A. Naberezhnov, S. Vakhrushev, B. Dorner, D. Strauch, and H. Moudden, Eur. Phys. J. B **11**, 13 (1999).